ISSN 1674-1056
http://cpb.iphy.ac.cn
http://iopscience.iop.org/cpb
中国物理 B
Chinese Physics
中国物理
Chinese Physics B

Influence factor analysis of field-free molecular orientation

Jing-Song Liu(刘劲松), Qi-Yuan Cheng(程起元), Da-Guang Yue(岳大光), Xu-Cong Zhou(周旭聪), Qing-Tian Meng(孟庆田)
Citation: Chin. Phys. B . 2018, 27(3): 033301. **doi:** 10.1088/1674-1056/27/3/033301

Journal homepage: http://cpb.iphy.ac.cn; http://iopscience.iop.org/cpb

What follows is a list of articles you may be interested in

Numerical analyses on optical limiting performances of chloroindium phthalocyanines with different substituent positions

Yu-Jin Zhang(张玉瑾), Xing-Zhe Li(李兴哲), Ji-Cai Liu(刘纪彩), Chuan-Kui Wang(王传奎)
Chin. Phys. B . 2016, 25(1): 013302. **doi:** 10.1088/1674-1056/25/1/013302

Interferences in photo-detached electron spectra froma non-collinear tri-atomic anion

A. Afaq, K. Farooq, M. A. Khan, Yi Xue-Xi
Chin. Phys. B . 2014, 23(10): 103304. **doi:** 10.1088/1674-1056/23/10/103304

Improved partial response maximum likelihood method combining modulation code for signal waveform modulation multi-level disc

Wang He-Qun, Pei Jing, Pan Long-Fa
Chin. Phys. B . 2014, 23(10): 104217. **doi:** 10.1088/1674-1056/23/10/104217

Field-free molecular orientation induced by combined femtosecond single- and dual-color laser pulses：The role of delay time and quantum interference

Qin Chao-Chao, Jia Guang-Rui, Zhang Xian-Zhou, Liu Yu-Fang, Long Jin-You, Zhang Bing
Chin. Phys. B . 2014, 23(1): 013302. **doi:** 10.1088/1674-1056/23/1/013302

An improved deconvolution method for X-ray coded imaging in inertial confinement fusion

Zhao Zong-Qing, He Wei-Hua, Wang Jian, Hao Yi-Dan, Cao Lei-Feng, Gu Yu-Qiu, Zhang Bao-Han
Chin. Phys. B . 2013, 22(10): 104202. **doi:** 10.1088/1674-1056/22/10/104202

Influence factor analysis of field-free molecular orientation*

Jing-Song Liu(刘劲松), Qi-Yuan Cheng(程起元), Da-Guang Yue(岳大光), Xu-Cong Zhou(周旭聪), and Qing-Tian Meng(孟庆田)†

School of Physics and Electronics, Shandong Normal University, Ji'nan 250358, *China*

(Received 25 October 2017; revised manuscript received 26 December 2017; published online 13 February 2018)

The effects of the characteristics of molecules and external fields on field-free molecular orientation are investigated through the comparison of HBr with LiH driven by the combination of a two-color laser pulse and a time-delayed THz laser pulse. It is shown that the dipole interaction has greater influence on field-free orientation than the hyperpolarizability interaction. In addition to the temperature dependence of orientation degree, the effects of the amplitudes of the two-color laser pulse and THz laser pulse, rising time, and THz laser frequency on molecular orientation are also discussed.

Keywords: molecular orientation, external fields, LiH, HBr

PACS: 33.80.–b, 42.50.–p, 33.20.Sn **DOI:** 10.1088/1674-1056/27/3/033301

1. Introduction

These years, due to the development of laser technology, the molecular alignment and orientation have aroused much interest both from physicists and chemists, thereby greatly promoting the development of relevant theoretical and experimental researches, such as multiphoton ionization,[1,2] high-order harmonic generation,[3–5] chemical reaction dynamics,[6,7] spectral manipulation,[8,9] and photoelectron angular distribution.[10–12] Alignment refers to the molecular axis along laboratory-fixed axes, while the orientation implies that the molecular axis has a specific "head-versus-tail" order. Molecular orientation and alignment can be obtained in adiabatic and nonadiabatic regimes. In the adiabatic regime, the molecular orientation and alignment generally exist in the time range of laser excitation, while for nonadiabatic regime, molecular orientation and alignment can be revived at the rotational period of the molecule, which is also called the field-free molecular orientation. When using a two-color laser pulse with a slow turn-on and rapid turn-off (STRT), the field-free molecular orientation also occurs when the pulse is over. In this case, if the maximal orientation degree does not change with time, it is also called the adiabatic process, while if the maximal orientation degree changes with time, it is called the nonadiabatic process.[13] The so-called field-free orientation occurs when the exciting pulses are over, so this idea has been widely used in such fields as molecular orbital imaging, ultrashort pulse diagnosis and control, etc.[14–17]

Compared with the molecular alignment, the field-free molecular orientation is very difficult to realize. Up to now, numerous research methods have been proposed to achieve molecular orientation. In the earlier studies, due to the combination effects of the permanent dipole interaction and the anisotropic polarizability interaction, the researchers found that using an intense laser field combined with a weak dc field, they can achieve field-free molecular orientation.[18,19] Although this method can effectively improve the molecular orientation, the presence of dc field may affect the measurement of orientation. In later studies, a two-color laser field[20–22] and a multi-color laser field[23–25] have been subsequently utilized to control the field-free molecular orientation via their interaction with molecular hyperpolarizability. However, because of the weak interaction between the laser and the molecular hyperpolarizability, improving the orientation degree needs high intensity of laser pulses, which may lead to the molecular ionization and dissociation.[26] Considering that the transition frequency between the molecular rotation levels is generally in the magnitude of THz, it is natural that the THz laser pulse can be used for realizing the field-free molecular orientation. In recent years, with the development of THz technology, the often used techniques including the half-cycle THz laser pulse (HCP),[27,28] single-cycle THz laser pulse[29,30] and few-cycle THz pulse,[31–33] have achieved good results of field-free molecular orientation.

Recently, the combination of non-resonant laser field and THz field is widely utilized for field-free molecular orientation. Compared with the previous methods, this combined field can obtain a higher degree of orientation, and more details about it can be found in Refs. [34]–[36]. According to the same idea, in this paper we take LiH and HBr for example to steer their field-free orientation by a two-color shaped laser pulse combined with a time-delayed THz laser pulse, investigate the effects of the characteristics of molecules and external fields on the field-free molecular orientation, and analyze

*Project supported by the National Natural Science Foundation of China (Grant No. 11674198), the Taishan Scholar Project of Shandong Province, China, and the Natural Science Foundation of Shandong Province, China (Grant No. ZR2014AM002).

†Corresponding author. E-mail: qtmeng@sdnu.edu.cn

© 2018 Chinese Physical Society and IOP Publishing Ltd

the experimental feasibility under present experimental conditions. After the theoretical frame about the orientation degree is introduced, in Section 3 we will firstly analyze the molecular orientation and its relation with the population of the rotational states by focusing on the molecular polarization characteristics under the same parameters of the laser field. Then, according to the different properties of these two molecules, we discuss the effects of some laser parameters such as rising time, two-color laser pulse intensity, THz field intensity, and THz frequency on molecular orientation. The effects of temperature on the orientations of different molecules are also discussed. Finally, the conclusions are drawn from the present study in Section 4.

2. Theoretical method

In the present scheme, a two-color laser pulse with a slow turn-on and rapid turn-off and a time-delayed THz laser pulse are employed to control the molecular orientation. The two-color laser pulse can be expressed as[37]

$$E_{\mathrm{STRT}}(t) = E_1(t)[\cos\omega_1 t + (\cos 2\omega_1 t)], \tag{1}$$

with

$$\begin{aligned} &E_1(t) = E_{01}\exp(-t^2/2\sigma^2), \\ &[\sigma = \sigma_{\mathrm{r}}(t \le 0), \quad \sigma = \sigma_f(t > 0), \quad \sigma_{\mathrm{r}} \gg \sigma_f], \end{aligned} \tag{2}$$

where E_{01} is the amplitude of STRT laser pulse, ω_1 and $2\omega_1$ are the fundamental frequency and the second harmonic frequency, σ_{r} and σ_f are the rising time and the falling time of the laser pulse, respectively. The THz laser pulse is given by

$$E_{\mathrm{THz}}(t) = E_2(t)\cos[\omega_{\mathrm{THz}}(t - t_{\mathrm{d}}) + \varphi], \tag{3}$$

with

$$E_2(t) = E_{02}\exp[-2\ln 2(t - t_{\mathrm{d}})^2/\tau^2], \tag{4}$$

where E_{02} is the electric field amplitude of the THz laser pulse, ω_{THz} the center frequency, τ the full width at half maximum (FWHM), t_{d} the delay time between two-color laser pulse and THz laser, and φ the carrier envelope phase.

In the rigid rotor approximation, the total Hamiltonian of the molecule interacting with the combination of two-color laser pulse and THz laser pulse is given by[38]

$$\begin{aligned} \hat{H}(t) \;=\; & B_{\mathrm{e}}\hat{J}^2 - \mu E_{\mathrm{THz}}(t)\cos\theta \\ & - \frac{1}{4}[(\alpha_\parallel - \alpha_\perp)\cos^2\theta + \alpha_\perp]E_1^2(t) \\ & - \frac{1}{8}[(\beta_\parallel - 3\beta_\perp)\cos^3\theta + 3\beta_\perp\cos\theta]E_1^3(t). \end{aligned} \tag{5}$$

The first term on the right-hand side of Eq. (5) denotes the molecular rotation energy, in which B_{e} is the molecular rotational constant, and $\hat{J}$ is the angular momentum operator. The second term is the dipole interaction between THz laser pulse and the molecule, where μ is the permanent dipole moment. The third and fourth terms are the interactions of a two-color laser pulse with the polarizability and hyperpolarizability of molecule, and can be obtained by using the rotating wave approximation due to the fast oscillation frequency of two-color laser pulse. The θ is the angle between the molecular axis and the polarization direction of the laser, $\alpha_\parallel(\beta_\parallel)$ and $\alpha_\perp(\beta_\perp)$ are the polarizabilities (hyperpolarizabilities) parallel and perpendicular to the molecular axis, respectively. The molecular orientation degree is defined as

$$\langle\cos\theta\rangle = \mathrm{Tr}\{\cos\theta\hat{\rho}(t)\}, \tag{6}$$

where Tr denotes the trace of a matrix and $\hat{\rho}(t)$ is the time-dependent density operator. The time evolution of the density operator can be obtained by solving the quantum Liouville equation,

$$\frac{\mathrm{d}\hat{\rho}(t)}{\mathrm{d}t} = -\frac{\mathrm{i}}{\hbar}[\hat{H}, \hat{\rho}(t)], \tag{7}$$

and the density operator $\hat{\rho}(t)$ can be expanded in the eigenstates of the rigid rotor Hamiltonian as[39]

$$\hat{\rho}(t) = \sum_{J,M,J',M'} \rho_{JMJ'M'}(t)\,|JM\rangle\langle J'M'|, \tag{8}$$

in which $\rho_{JMJ'M'}(t)$ are determined by coupling differential equations[40]

$$\begin{aligned} &\frac{\mathrm{d}\rho_{JMJ'M'}(t)}{\mathrm{d}t} \\ &= -\frac{\mathrm{i}}{\hbar}\{(\varepsilon_J - \varepsilon_{J'})\rho_{JMJ'M'}(t) \\ &\quad - \mu\mathrm{E}_{\mathrm{THZ}}(t)\sum_{J_1M_1}[\rho_{J_1M_1J'M'}(t)V^{(1)}_{JMJ_1M_1} \\ &\quad - \rho_{JMJ_1M_1}(t)V^{(1)}_{J_1M_1J'M'}] \\ &\quad - \frac{1}{4}\mathrm{E}_1^2(t)\Delta\alpha\sum_{J_1M_1}[\rho_{J_1M_1J'M'}(t)V^{(2)}_{JMJ_1M_1} \\ &\quad - \rho_{JMJ_1M_1}(t)V^{(2)}_{J_1M_1J'M'}] \\ &\quad - \frac{1}{8}\mathrm{E}_1^3(t)\sum_{J_1M_1}[(\beta_\parallel - 3\beta_\perp)(\rho_{J_1M_1J'M'}(t)V^{(3)}_{JMJ_1M_1} \\ &\quad - \rho_{JMJ_1M_1}(t)V^{(3)}_{J_1M_1J'M'}) \\ &\quad + 3\beta_\perp(\rho_{J_1M_1J'M'}(t)V^{(1)}_{JMJ_1M_1} - \rho_{JMJ_1M_1}(t)V^{(1)}_{J_1M_1J'M'})]\}, \end{aligned} \tag{9}$$

where $V^{(i)}_{JMJ'M'} = \langle JM|\cos^i\theta|J'M'\rangle$ $(i = 1,2,3)$. The above equation is solved by utilizing the fourth-order Runge–Kutta method. The initial density operator satisfies the temperature-dependent Boltzmann distribution,

$$\rho_0(T) = \frac{1}{Z}\sum_{J=0}^{\infty}\sum_{M=-J}^{M=J}|JM\rangle\langle JM|\,\mathrm{e}^{-B_{\mathrm{e}}J(J+1)/K_{\mathrm{B}}T}, \tag{10}$$

where

$$Z = \sum_{J=0}^{\infty} \sum_{M=-J}^{M=J} \mathrm{e}^{-B_{\mathrm{e}}J(J+1)/K_{\mathrm{B}}T} \tag{11}$$

is the partition function, with K_{B} being the Boltzmann constant, and T being temperature.

3. Results and discussion

In this calculation, we take LiH and HBr for example to study the effects of the characteristics of molecules and external fields on their field-free orientation. The parameters in the calculation are summarized in Table 1.[41–43] Obviously, the quantities of the rotational constant and polarizability for these two molecules are very close to each other, but the hyperpolarizabilities and dipole moments are quite different.

The parameters of the two-color laser pulse are taken to be $E_{01} = 1.0 \times 10^8$ V·cm^{-1}, $\sigma_{\mathrm{r}} = 2$ ps, $\sigma_{\mathrm{f}} = 0.4$ ps, and $\omega_{\mathrm{l}} = 12500$ cm^{-1}, and the parameters of THz laser pulse are $E_{02} = 2.0 \times 10^5$ V·cm^{-1}, $t_{\mathrm{d}} = 2.2$ ps, $\varphi = \pi$, $\omega_{\mathrm{THz}} = 18$ cm^{-1}, $\tau = 1$ ps, and $T = 0$ K. Figure 1 shows the time evolutions of the molecular orientations of LiH and HBr steered by the THz laser pulse, the two-color laser pulse, and a combination of the two laser pulses. As can be seen, the molecular orientation repeatedly revives around $t = nT_{\mathrm{rot}}$ $(n = 0, 1, 2, \ldots)$, where $T_{\mathrm{rot}} = h/2B_{\mathrm{e}}$ is the rotational period. Obviously, because of their similar rotational constants, the rotational periods of these two molecules are also very close to each other, which gives almost the same repeatedly revival time of the orientation. However due to the fact that LiH possesses larger dipole moment and polarizability as well as the hyperpolarizability, it has a higher degree of orientation than HBr under the same laser conditions. Certainly for both LiH and HBr, their hyperpolarization interactions are weak, so the field-free orientation is mainly provided by the dipole interaction.

Table 1. Molecular parameters of LiH and HBr for numerical computation.

Molecules	B_{e}/cm^{-1}	μ/D	$\alpha_{\parallel}$/Å^3	$\alpha_{\perp}$/Å^3	$\beta_{\parallel}$/Å^5	$\beta_{\perp}$/Å^5
LiH	7.52	5.87	3.82	4.38	5.44×10^{10}	2.021×10^{10}
HBr	8.348	0.83	3.64	3.315	-1.07×10^{9}	4.3×10^{8}

Under the combined fields, the two-color shaped laser pulse firstly induces a non-resonant excitation, after a delay time the THz laser pulse induces a resonant transition. The rotational populations of molecules LiH and HBr steered by the combination of the two laser pulses are shown in Figs. 2(a) and 2(b). Obviously, before excitation both LiH and HBr populate at $J = 0$, then under the stimulation of the combined field, the rotational population displays a Rabi-type changing, and after the pulse the population does not change with time. The periodic field-free molecular orientation shown in Fig. 1 can be explained by the fact that a coherent rotational wave packet is produced after the interaction between the combined fields and molecules, which suffers a periodic dephasing and rephasing when evolving freely in time, i.e., the collapsed wave packet is periodically reconstructed at multiple revival times.[44] After the interaction the populated rotational states of LiH are almost of $J = 0, 1, 2$ and the corresponding populations are 0.442, 0.327, and 0.229, while the populated rotational states of HBr are almost of $J = 0$, 1, and the corresponding populations are 0.899 and 0.095. According to the uncertainty principle $\Delta J \cdot \Delta\theta \geq \hbar/2$, where ΔJ is the difference in the number of the occupied rotational states between before and after the laser pulse, since a better field-free molecular orientation requires a narrower $\Delta\theta$, a broad rotational band ΔJ is required.[45] We can see that because of the larger dipole moment and hyperpolarizability, LiH has a broader rotational band, so it has a higher degree of orientation after driven by laser pulse (see Fig. 1).

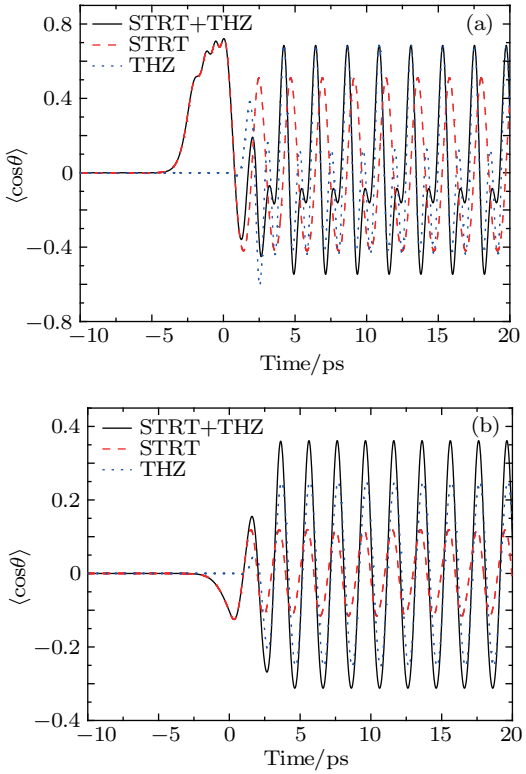


Fig. 1. (color online) Time evolutions of the molecular orientations of (a) LiH and (b) HBr steered by the THz laser pulse (dotted) , the two-color laser pulse (dashed), and a combination of the two laser pulses (solid), where $E_{01} = 1.0 \times 10^8$ V·cm^{-1}, $\sigma_{\mathrm{r}} = 2$ ps, $\sigma_{\mathrm{f}} = 0.4$ ps, $\omega_{\mathrm{l}} = 12500$ cm^{-1}, $E_{02} = 2.0 \times 10^5$ V·cm^{-1}, $t_{\mathrm{d}} = 2.2$ ps, $\tau = 1$ ps, $\varphi = \pi$, $\omega_{\mathrm{THz}} = 18$ cm^{-1}, and $T = 0$ K.

To illustrate the influence of the rising time of the two-color laser pulse on molecular orientation, we show the maxima of molecular orientation $\langle\cos\theta\rangle_{\max}$ of LiH and HBr with the rising time σ_{r} in Fig. 3. For LiH, $\langle\cos\theta\rangle_{\max}$ initially increases from 0.65 to 0.71 as time rises from 1.2 to 2 ps, and then decreases from 0.71 to 0.69 with time rising. Finally, $\langle\cos\theta\rangle_{\max}$ converges to a constant value of 0.70 after 4 ps.

Obviously in the time interval from 1.2 ps to 4 ps, the molecular orientation undergoes a nonadiabatic process. However, when the rising time increases from 4.1 ps to 20 ps, the interaction time increases from $2T_{\rm rot}$ to $10T_{\rm rot}$, and the rising time is long enough to ensure that the molecular orientation is near an adiabatic process. By using this shaped laser pulse, we can see that the field-free molecular orientation undergoes an adiabatic process. For HBr, when the rising time increases from 1.2 ps to 6 ps, the molecular orientation can be viewed as a nonadiabatic process. However, when the rising time increases from 6.1 ps to 20 ps, the molecular orientation arrives at a saturation state, which is nearly an adiabatic process. Thus, due to the fact that LiH and HBr have nearly the same repeatedly revival time of the orientation, they reach their stages of adiabatic process in a similar rising time. But because of their difference in hyperpolarizability, the field–molecule interaction can change their rotational states in a respective strength, which leads to different nonadiabatic processes, so there is a peak-like changing for LiH molecule.

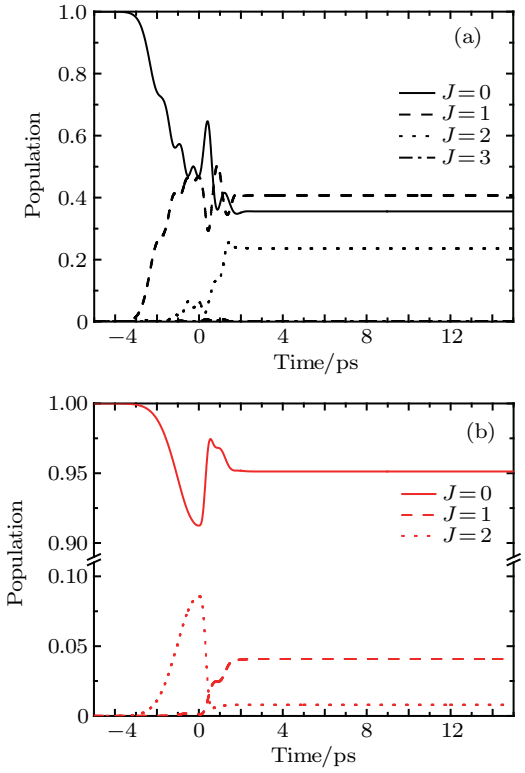


Fig. 2. (color online) Time evolutions of rotational population for (a) LiH and (b) HBr, respectively. The pulse parameters are the same as those in Fig. 1.

In order to expound the influence of two-color field intensity on molecular orientation, we show the plots of maximal orientation degree $\langle\cos\theta\rangle_{\rm max}$ versus intensity of the two-color laser pulse for LiH and HBr in Fig. 4(a). For LiH, with the intensity of the two-color field increasing from 1.0×10^7 V·cm^{-1} to 4.5×10^7 V·cm^{-1}, $\langle\cos\theta\rangle_{\rm max}$ increases from 0.72 to 0.76 , then decreases from 0.76 to 0.64 as the intensity increases from 4.5×10^7 V·cm^{-1} to 1.4×10^8 V·cm^{-1}. While for HBr, as the intensity of the two-color field increases from 1.0×10^7 V·cm^{-1} to 1.4×10^8 V·cm^{-1}, $\langle\cos\theta\rangle_{\rm max}$ first increases from 0.26 to 0.6, then decreases from 0.6 to 0.55. This phenomenon of first increasing and then decreasing for the orientations of both HBr and LiH can be explained by their undergoing nonadiabatic processes at $\sigma_{\rm r}=4$ ps. In addition,

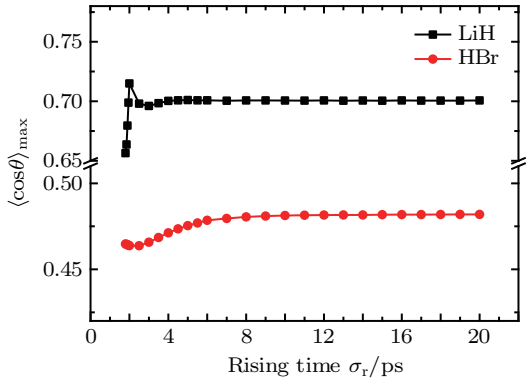


Fig. 3. (color online) Plots of maximal orientation degree $\langle\cos\theta\rangle_{\rm max}$ versus rising time $\sigma_{\rm r}$ of LiH (black line) and HBr (red line) at $E_{02}=9.0\times10^5$ V·cm^{-1}. The other pulse parameters are the same as those in Fig. 1.

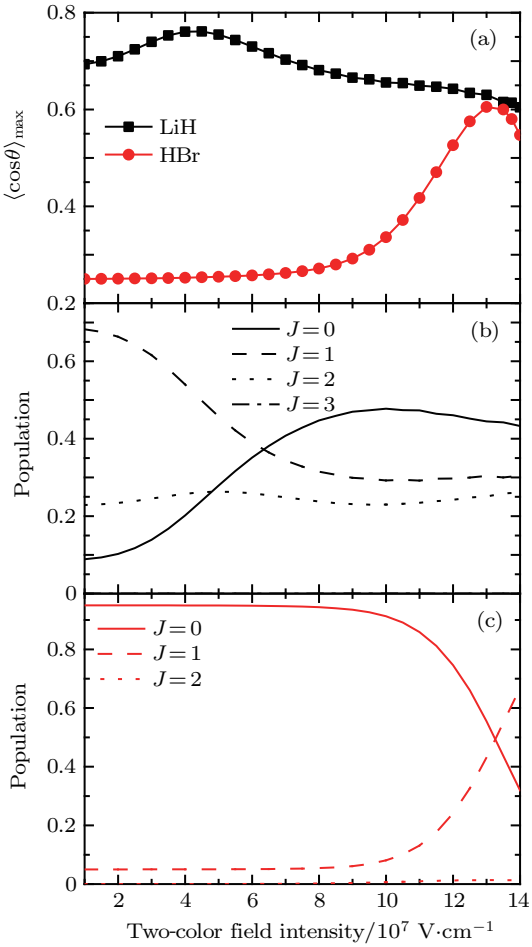


Fig. 4. (color online) (a) Plots of maximal orientation degree $\langle\cos\theta\rangle_{\rm max}$ versus the amplitude of the two-color laser pulse of LiH (black line) and HBr (red line). Plots of rotational population versus amplitude of the two-color laser pulse for (b) LiH and (c) HBr after laser pulse, respectively. The parameters are the same as those in Fig. 1 except for $\sigma_{\rm r}=4$ ps.

the increase in the two-color field amplitude may change the rotational structure, leading to the different populations of rotational states as shown in Figs. 4(b) and 4(c), which is the reason why the peak of the $\langle\cos\theta\rangle_{\max}$ appears at different amplitudes, and the highest value for $\langle\cos\theta\rangle_{\max}$ occurs when the occupied rotational states have relatively small difference. Furthermore, due to the larger hyperpolaizability, LiH is more sensitive to the two-color field than HBr.

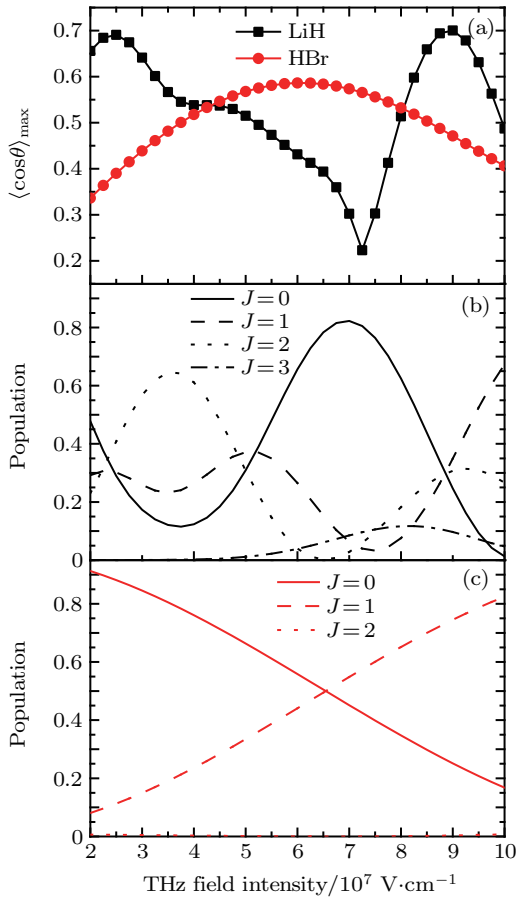


Fig. 5. (color online) (a) Plots of maximal orientation degree $\langle\cos\theta\rangle_{\max}$ versus the amplitude of the THz laser pulse with $\sigma_r = 4$ ps , $E_{01} = 1.0\times10^8$ V·cm^{-1}, $\omega_{THz} = 18$ cm^{-1}, and $T = 0$ K. The plots of rotational population versus the amplitude of the THz laser pulse for (b) LiH (b) and (c) HBr, respectively.

In the above analysis, we find that the two-color field intensity has an influence on molecular orientation, so we further investigate the influence of the THz pulse intensity on molecular orientation. Figure 5(a) illustrates the variations of the maximal orientation degree $\langle\cos\theta\rangle_{\max}$ with the increase in the amplitude of THz laser pulse for LiH and HBr. For HBr which has a smaller dipole moment, when THz field amplitude changes from 2.0×10^5 V·cm^{-1} to 1.0×10^6 V·cm^{-1}, $\langle\cos\theta\rangle_{\max}$ first increases and then decreases, and the peak of the $\langle\cos\theta\rangle_{\max}$ occurs at an intensity of about 6.0×10^5 V·cm^{-1}.While for LiH, when THz field amplitude changes from 2.0×10^5 V·cm^{-1} to 1.0×10^6 V·cm^{-1}, $\langle\cos\theta\rangle_{\max}$ has an irregular oscillation, and the two peaks occur at 2.0×10^5 V·cm^{-1} and 9.0×10^5 V·cm^{-1}, respectively. This is because different THz field intensity leads to different population of rotational states, as shown in Figs. 5(b) and 5(c), thus leading to different coherent superposition of wave functions. Because LiH has a larger dipole moment, it is much easier to be affected by the THz pulse. It is necessary to point out that the maximal electric field intensity of THz laser pulse, which is generated by adjusting the polarization of the two-color laser pulses, can be larger than 1.0×10^6 V·cm^{-1}, so the above condition is easy to meet experimentally.[46,47]

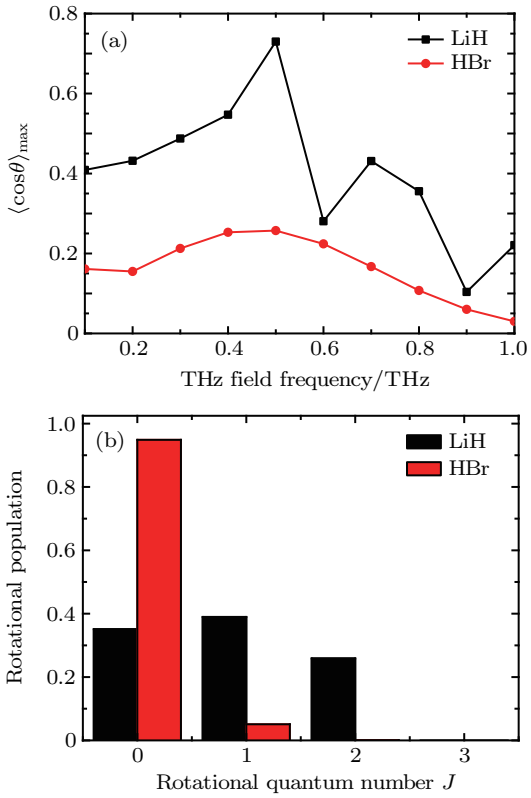


Fig. 6. (color online) (a) Variations of maximal orientation degree of LiH (black) and HBr (red) with THz field frequency, where $E_{01} = 6.0\times10^7$ V·cm^{-1}, $E_{02} = 2.0\times10^5$ V·cm^{-1}, $\sigma_r = 4$ ps, $T = 0$ K. (b) Populations of rotational states of LiH and HBr at $\omega_{THz} = 0.5$ THz with other parameters being the same as those in panel (a).

To elucidate the effect of THz frequency on molecular orientation, we display the plots of maximal orientation degree $\langle\cos\theta\rangle_{\max}$ versus THz field frequency for LiH and HBr in Fig. 6(a). From Fig. 6(a), we can see that the highest values of $\langle\cos\theta\rangle_{\max}$ for both LiH and HBr appear at THz field frequency about 0.5 THz (18 cm^{-1}). This is because the interaction between the THz field and the molecules is a resonant interaction, and the resonance transition frequency between molecular levels is $\Delta\omega_{J,J+1} = 2B_e(J+1)/\hbar = 2\pi\omega_{THz}$. For HBr, the resonant transition frequency from $J = 0$ to $J = 1$ state is $\Delta\omega_{0,1} = 2\pi\times0.52$ THz, while for LiH, the resonant transition frequency from $J = 0$ to $J = 1$ state is $\Delta\omega_{0,1} = 2\pi\times0.48$ THz, so the highest values of $\langle\cos\theta\rangle_{\max}$ both appear at the frequency about 0.5 THz viewed from the figure. From Fig. 6(b), we can see that the populated rotational states of HBr at $\omega_{THz} = 0.5$ THz are almost of $J = 0, 1,$

while for LiH the populated rotational states are of $J = 0, 1, 2$, and $J = 1$ state has the largest population. The above results show that an efficient molecular orientation can be achieved by using the proper frequency of the THz field.

It is necessary to point out that the above calculations are performed at temperature $T = 0$ K. However, in the actual experiments, the molecular ensemble is at a finite temperature. In order to illustrate the effect of temperature, we show the time evolutions of molecular orientation of LiH and HBr at $T = 0$ K, 10 K, and 20 K in Figs. 7(a) and 7(b), respectively. For LiH, the maximal orientations at $T = 0$, 10, and 20 K are 0.655, 0.461, and 0.244, while for HBr at $T = 0$, 10, and 20 K, the maximal orientations are 0.336, 0.237, and 0.113. As shown in Figs. 7(c)–7(f), both LiH and HBr populate the higher rotational states at higher temperatures before excitation, but during excitation the influence of the combined field is smaller, so leading to ΔJ decreasing with temperature increasing. As a consequence, the increase of the temperature can lead to the decrease of the degree of maximal molecular orientation. With the development of the ultracold technique, the temperature realized can be very near 0 K ($\sim$ μK), so it is possible to achieve the highest degree of molecular orientation.[48]

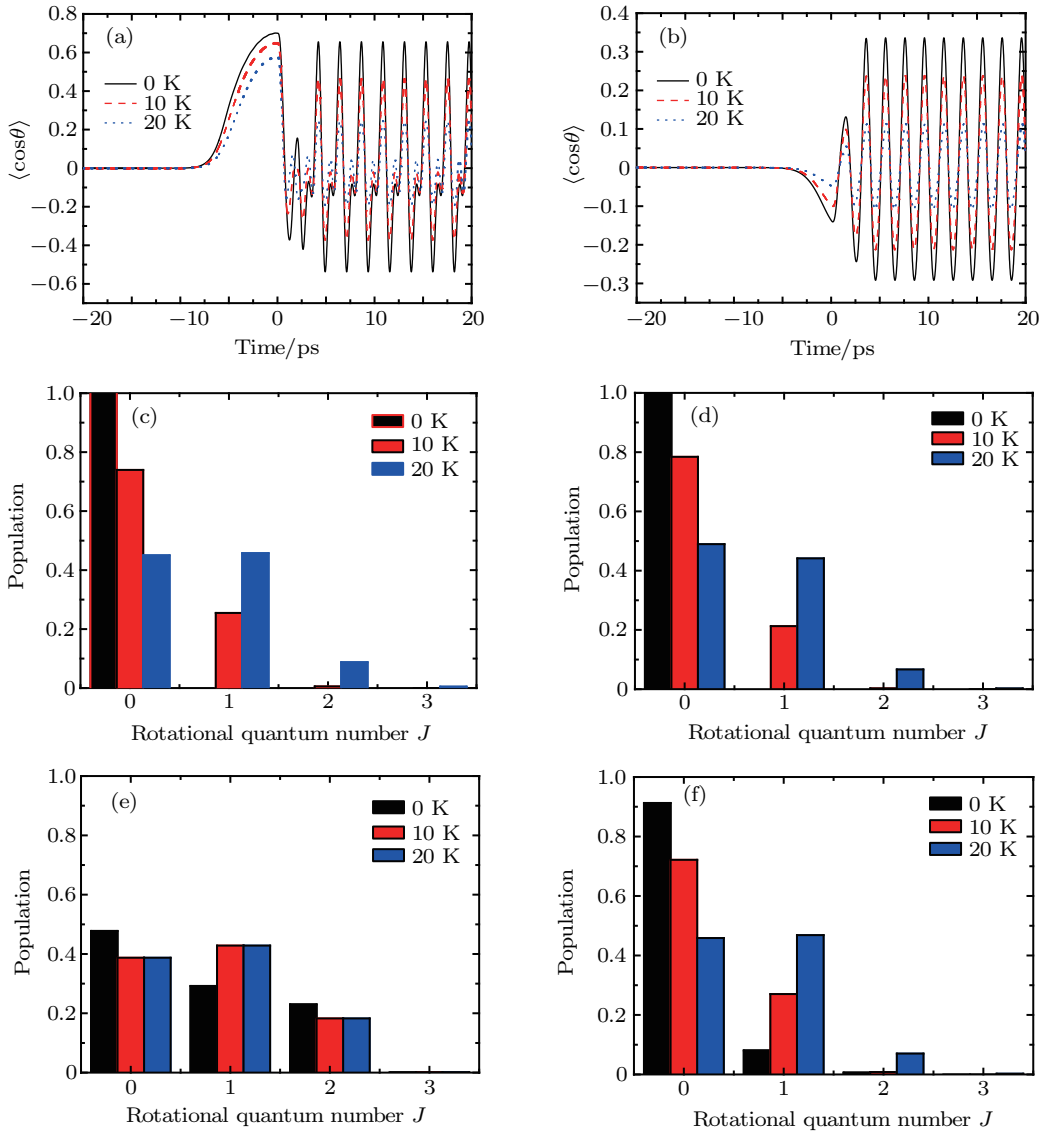


Fig. 7. (color online) Time evolution of molecular orientations of (a) LiH and (b) HBr at $T = 0$ K (solid line), 10 K (dash line), and 20 K (dotted line), ((c), (d)) corresponding rotational population before excitation, and ((e), (f)) the corresponding rotational population after excitation. The parameters are adopted to be $\sigma_r = 4$ ps, $\omega_{THz} = 18$ cm^{-1}, $E_{01} = 1.0 \times 10^8$ V·cm^{-1}, and $E_{02} = 2.0 \times 10^5$ V·cm^{-1}.

4. Conclusions

We analyze the effects of the characteristics of molecules and external fields on field-free molecular orientation by comparing HBr with LiH molecules driven by the combination of a two-color laser pulse with time-delayed THz laser pulse in this work. It is shown that the dipole interaction has greater influence on field-free orientation than the hyperpolarizability interaction. Because of the similar repeated revival times, HBr

and LiH reach the adiabatic process at almost the same rising time. Taking advantage of the different characteristics of molecules, an efficient molecular orientation can be achieved by using the proper two-color field intensity, THz field intensity and frequency. The different rotational populations caused by the fields are the reason for producing different values of $\langle\cos\theta\rangle_{\max}$. The temperature effects of HBr and LiH on molecular orientation are almost the same, i.e., with the rising temperature, the molecular orientation degree decreases rapidly. We hope that this study can provide some information for experimentalists to explain the relevant results.

References

[1] Suzuki T, Minemoto S, Kanai T and Sakai H 2004 *Phys. Rev. Lett.* **92** 133005
[2] Zeidler D, Staudte A, Bardon A B, Villeneuve D M, Dörner R and Corkum P B 2005 *Phys. Rev. Lett.* **95** 203003
[3] Kanai T, Minemoto S and Sakai H 2005 *Nature* **435** 470
[4] Miyazaki K, Kaku M, Miyaji G, Abdurrouf A and Faisal F H 2005 *Phys. Rev. Lett.* **95** 243903
[5] Kanai T, Minemoto S and Sakai H 2007 *Phys. Rev. Lett.* **98** 053002
[6] Hu J, Wang M S, Han K L and He G Z 2006 *Phys. Rev. A* **74** 063417
[7] Hu J, Han K L and He G Z 2005 *Phys. Rev. Lett.* **95** 123001
[8] Liu J, Feng Y H, Li H, Lu P F, Pan H F, Wu J and Zeng H P 2011 *Opt. Express* **19** 40
[9] Li H, Li W X, Feng Y H, Liu J, Pan H F and Zeng H P 2012 *Phys. Rev. A* **85** 052515
[10] Holmegaard L, Hansen J L, Kalhøj L, Kragh S L, Stapelfeldt H, Filsinger F, Küpper J, Meijer G, Dimitrovski D, Abu-samha M, Martiny C P J and Madsen L B 2010 *Nat. Phys.* **6** 428
[11] Hansen J L, Stapelfeldt H, Dimitrovski D, Abu-Samha M, Martiny C P and Madsen L B 2011 *Phys. Rev. Lett.* **106** 073001
[12] Yang X D, Gao M and Tian Y 2016 *Chin. Phys. Lett.* **33** 013102
[13] Rosca-Pruna F and Vrakking M J J 2001 *Phys. Rev. Lett.* **87** 153902
[14] Itatani J, Levesque J, Zeidler D, Niikura H, Pepin H, Kieffer J C, Corkum P B and Villeneuve D M 2004 *Nature* **432** 867
[15] Zhao Z Y, Han Y C, Yu J and Cong S L 2014 *J. Chem. Phys.* **140** 044316
[16] Wang B B, Han Y C and Cong S L 2015 *J. Chem. Phys.* **143** 094303
[17] Wang Y, Yue D G, Zhou X C, Guo Y H and Meng Q T 2017 *Chin. Phys. B* **26** 043202
[18] Friedrich B and Herschbach D 1999 *J. Chem. Phys.* **111** 6157
[19] Friedrich B and Herschbach D 1999 *J. Phys. Chem. A* **103** 10280
[20] Wu J and Zeng H P 2010 *Phys. Rev. A* **81** 053401
[21] Zhang S A, Lu C H, Jia T Q, Wang Z G and Sun Z R 2011 *J. Chem. Phys.* **135** 034301
[22] Qin C C, Zhao X D, Zhang X Z and Liu Y F 2013 *Chin. Phys. Lett.* **30** 023302
[23] Zhang S A, Shi J H, Zhang H, Jia T Q, Wang Z G and Sun Z R 2011 *Phys. Rev. A* **83** 023416
[24] Xu S W, Yao Y H, Lu C H, Jia T Q, Ding J X, Zhang S A and Sun Z R 2014 *Phys. Rev. A* **90** 033416
[25] Huang Z Y, Wang D, Zheng L, Li W K, Zhao R R and Leng Y X 2017 *Chin. Phys. B* **26** 054209
[26] Frumker E, Hebeisen C T, Kajumba N, Bertrand J B, Worner H J, Spanner M, Villeneuve D M, Naumov A and Corkum P B 2012 *Phys. Rev. Lett.* **109** 113901
[27] Machholm M and Henriksen N E 2001 *Phys. Rev. Lett.* **87** 193001
[28] Shu C C, Yuan K J, Hu W H, Yang J and Cong S L 2008 *Phys. Rev. A* **78** 055401
[29] Shu C C and Henriksen N E 2013 *Phys. Rev. A* **87** 013408
[30] Zhao Z Y, Han Y C, Huang Y and Cong S L 2013 *J. Chem. Phys.* **139** 044305
[31] Shu C C, Yuan K J, Hu W H and Cong S L 2009 *Phys. Rev. A* **80** 011401
[32] Qin C C, Tang Y, Wang Y M and Zhang B 2012 *Phys. Rev. A* **85** 053415
[33] Qin C C, Liu Y Z, Zhang X Z and Liu Y F 2013 *Chin. Phys. Lett.* **30** 023301
[34] Kitano K, Ishii N and Itatani J 2011 *Phys. Rev. A* **84** 053408
[35] Huang Y, Xie T, Li J, Yu J and Cong S L 2014 *Laser Phys.* **24** 016002
[36] Li H, Li W X, Feng Y H, Pan H F and Zeng H P 2013 *Phys. Rev. A* **88** 013424
[37] Muramatsu M, Hita M, Minemoto S and Sakai H 2009 *Phys. Rev. A* **79** 011403
[38] Liu Y, Li J, Yu J and Cong S L 2013 *Laser Phys. Lett.* **10** 076001
[39] Ramakrishna S and Seideman T 2005 *Phys. Rev. Lett.* **95** 113001
[40] Ramakrishna S and Seideman T 2006 *J. Chem. Phys.* **124** 034101
[41] Pecul M 2005 *Chem. Phys. Lett.* **404** 217
[42] Yun H, Kim H T, Kim C M, Nam C H and Lee J 2011 *Phys. Rev. A* **84** 065401
[43] Bishop D M and Norman P 1999 *J. Chem. Phys.* **111** 3042
[44] Torres R, de Nalda R and Marangos J P 2005 *Phys. Rev. A* **72** 023420
[45] Shu C C, Yuan K J, Hu W H and Cong S L 2010 *J. Chem. Phys.* **132** 244311
[46] Minami Y, Kurihara T, Yamaguchi K, Nakajima M and Suemoto T 2013 *Appl. Phys. Lett.* **102** 041105
[47] Oh T I, You Y S, Jhajj N, Rosenthal E W, Milchberg H M and Kim K Y 2013 *New J. Phys.* **15** 075002
[48] Quemener G and Julienne P S 2012 *Chem. Rev.* **112** 4949